Hindawi Publishing Corporation
Journal of Nanomaterials
Volume 2014, Article ID 972869, 6 pages
http://dx.doi.org/10.1155/2014/972869

Research Article

Enhanced Performance of $Mg_{0.1}Zn_{0.9}O$ UV Photodetectors Using Photoelectrochemical Treatment and Silica Nanospheres

Hsin-Ying Lee,[1] Yu-Chang Lin,[1] Meng-Ju Lee,[2] Wu-Yih Uen,[2] and Kondepudy Sreenivas[3]

[1] *Department of Photonics, Advanced Optoelectronic Technology Center, National Cheng Kung University, Tainan 701, Taiwan*
[2] *Department of Electronic Engineering, Chung Yuan Christian University, Chung Li 320, Taiwan*
[3] *Department of Physics and Astrophysics, University of Delhi, Delhi110007, India*

Correspondence should be addressed to Hsin-Ying Lee; hylee@ee.ncku.edu.tw

Received 11 December 2013; Revised 24 January 2014; Accepted 24 January 2014; Published 5 March 2014

Academic Editor: Sheng-Po Chang

The $Mg_{0.1}Zn_{0.9}O$ films were grown using atomic layer deposition (ALD) system and applied to metal-semiconductor-metal ultraviolet photodetectors (MSM-UPDs) as an active layer. To suppress the dangling bonds on the $Mg_{0.1}Zn_{0.9}O$ surface, the photoelectrochemical (PEC) treatment was used to passivate the $Mg_{0.1}Zn_{0.9}O$ surface, which could reduce the dark current of the MSM-UPDs about one order. Beside, to increase more incident light into the $Mg_{0.1}Zn_{0.9}O$ active layer of the MSM-UPDs, the 500-nm-diameter silica nanospheres were spin-coated on the $Mg_{0.1}Zn_{0.9}O$ active layer to improve the antireflection capability at the wavelength of 340 nm. The reflectivity of the $Mg_{0.1}Zn_{0.9}O$ films with silica nanospheres antireflection layer decreased about 7.0% in comparison with the $Mg_{0.1}Zn_{0.9}O$ films without silica nanospheres. The photocurrent and UV-visible ratio of the passivated $Mg_{0.1}Zn_{0.9}O$ MSM-UPDs with antireflection layer were enhanced to 5.85 μA and 1.44×10^4, respectively, at the bias voltage of 5 V. Moreover, the noise equivalent power and the specific detectivity of the passivated $Mg_{0.1}Zn_{0.9}O$ MSM-UPDs with antireflection layer were decreased to 2.60×10^{-13} W and increased to 1.21×10^{12} cmHz$^{1/2}$W^{-1}, respectively, at the bias voltage of 5 V. According to the above mentions, the PEC treatment and silica nanospheres antireflection layer could effectively enhance the performance of $Mg_{0.1}Zn_{0.9}O$ MSM-UPDs.

1. Introduction

Ultraviolet (UV) photodetectors have received more attention due to their wide applications, such as flame detection, chemical agent detection, space communications, and solar astronomy [1–3]. Different kinds of UV photodetectors have been developed to fit the requirements for various applications. To fabricate UV and deep UV photodetectors, the ternary magnesium zinc oxide ($Mg_xZn_{1-x}O$) with the wide bandgap is a promising candidate. Owing to the fact that the ionic radius of Mg^{2+} (0.57 Å) is very close to that of Zn^{2+} (0.6 Å), the $Mg_xZn_{1-x}O$ alloy with Mg content $x = 0.36$ remains a single phase wurtzite structure [4]. Recently, several researches reported that $Mg_xZn_{1-x}O$ films were prepared by various techniques, such as molecular beam epitaxy (MBE) [5, 6], metal organic chemical vapor deposition (MOCVD) [7, 8], magnetron radio frequency (RF) sputtering [9, 10], vapor cooling condensation system [11], and pulsed laser deposition (PLD) [12, 13]. In this work, the high quality $Mg_{0.1}Zn_{0.9}O$ films were deposited using an atomic layer deposition (ALD) and applied in the metal-semiconductor-metal ultraviolet photodetectors (MSM-UPDs). Since the surface states on the $Mg_xZn_{1-x}O$ surface seriously affected the performance of the MSM-UPDs, how to improve the surface states was the primary issue. There were some methods, such as hydrogen peroxide treatment [14], $(NH_4)_2S_x$ treatment [15], and photoelectrochemical (PEC) treatment [16] that were used to passivate the $Mg_xZn_{1-x}O$ surface. In this work, the PEC treatment was used to passivate the $Mg_{0.1}Zn_{0.9}O$ surface to decrease the dangling bond on the $Mg_{0.1}Zn_{0.9}O$ surface, which could reduce the surface states and improve the performance of the MSM-UPDs. Moreover, to further enhance the performance of the detectors, the antireflection technique was applied to increase the amount of light incident into the active layer of the MSM-UPDs. Many approaches were used to deposit

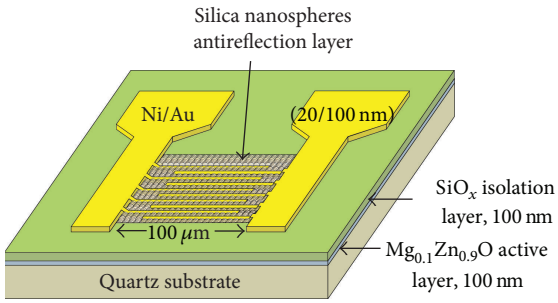

Figure 1: The schematic configuration of $Mg_{0.1}Zn_{0.9}O$ MSM-UPDs with silica nanospheres antireflection layer.

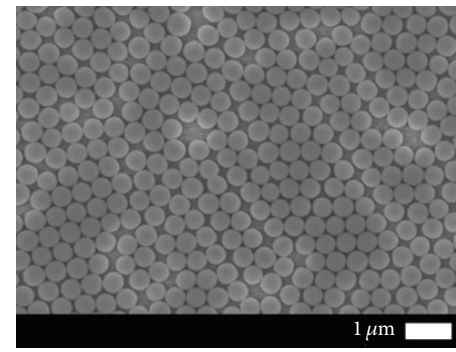

Figure 2: The surface morphology of the 500 nm-diameter silica nanospheres antireflection layer.

the antireflection layers, such as magnetron RF sputtering [17], electron-beam evaporator [18], lithography technologies [19], phase-separation [20], and self-assembled technology [21]. Among these, the self-assembled technology had some advantages: low cost, easier preparation, and low deposition temperature. In this work, the self-assembled technology was used to form a self-assembled silica nanosphere layer as an antireflection layer for the $Mg_{0.1}Zn_{0.9}O$ MSM-UPDs. The performance enhancement of the $Mg_{0.1}Zn_{0.9}O$ MSM-UPDs using PEC treatment and an antireflection nanosphere layer was investigated.

2. Experimental Procedures

Figure 1 shows the schematic configuration of the $Mg_{0.1}Zn_{0.9}O$ MSM-UPDs with silica nanospheres antireflection layer. The 100 nm-thick $Mg_{0.1}Zn_{0.9}O$ films were deposited on the quartz substrates using an ALD system. The precursors of diethylzinc (DEZn), bis (cyclopentadienyl) magnesium (Cp_2Mg), and water (H_2O) were used as zinc (Zn), magnesium (Mg), and oxygen (O) sources, respectively. The chamber pressure and the substrate temperature were fixed at 0.6 torr and 100°C, respectively. The pulse time of DEZn, Cp_2Mg, and H_2O was 0.5 s, 2 s, and 1 s, respectively. After each step of reactant, argon (Ar) gas was utilized as the carrier gas for 3 s. In the ALD system, the Mg content of the $Mg_xZn_{1-x}O$ film was varied by changing the cycle ratio of ZnO to MgO. In this work, the $Mg_{0.1}Zn_{0.9}O$ film was repeatedly deposited by stacking nine ZnO cycles and one MgO cycle. In the deposited procedure, the ZnO cycle was the end cycle. The composition of $Mg_xZn_{1-x}O$ film was measured by the energy dispersive spectrometer (EDS), and the content (x) of Mg was estimated to be 0.1. The optical energy bandgap of the resultant $Mg_{0.1}Zn_{0.9}O$ film was estimated to be 3.65 eV using the transmission spectrum. To fabricate MSM-UPDs, the active region of $100 \times 100\,\mu m^2$ was defined by conventional photolithography and lift-off technique, and then a 100 nm-thick SiO_x isolation layer was deposited by a magnetron RF sputtering. Prior to the interdigital metal deposition, the surface of active region was passivated using the PEC treatment to decrease surface states and dangling bonds. In the PEC treatment processes, the MSM-UPDs were dipped in the ammonia (NH_4OH) electrolytic solution with a pH value of 8.6 and illuminated by He-Cd laser with the wavelength of 325 nm and power density of 10 mW/cm^2 for 90 s. The interdigital Schottky metals Ni/Au (20 nm/100 nm) were immediately deposited on the $Mg_{0.1}Zn_{0.9}O$ active layer with PEC treatment using an electron-beam evaporator. Both the width and spacing of the metal fingers were 2 μm. Finally, the silica nanospheres with 500 nm diameter were coated on the surface of MSM-UPDs as the antireflection layer using a self-assembled technology. The coating procedure of silica nanospheres included that the rotational speed was 300 rpm for 60 s and then the rotational speed immediately increased to 3000 rpm for 30 s. The surface morphology of the 500 nm-diameter silica nanospheres coated layer on $Mg_{0.1}Zn_{0.9}O$ films deposited on the quartz substrates was observed by scanning electron microscopy (SEM) and is shown in Figure 2. It can be seen that the silica nanoparticles coated layer was a uniform single layer. The electrical characteristics of the $Mg_{0.1}Zn_{0.9}O$ MSM-UPDs were characterized by Agilent 4156 C semiconductor parameter analyzer. The photoresponsivity spectra of the $Mg_{0.1}Zn_{0.9}O$ MSM-UPDs were measured using a monochromator and an Xe lamp source.

3. Results and Discussion

To understand the function of the PEC treatment, the current-voltage (I-V) characteristic of the $Mg_{0.1}Zn_{0.9}O$ MSM-UPDs with and without PEC treatment was measured and is shown in Figure 3. At bias voltage of 5 V, the dark current of the resultant MSM-UPDs with and without PEC treatment was 0.15 nA and 1.66 nA, respectively. The dark current of the passivated $Mg_{0.1}Zn_{0.9}O$ MSM-UPDs was lower than that of the unpassivated $Mg_{0.1}Zn_{0.9}O$ MSM-UPDs for all applied voltages. In general, the dark current was probably influenced by the surface condition. Since the $Mg_{0.1}Zn_{0.9}O$ film deposited using ALD system, some dangling bonds remained on the $Mg_{0.1}Zn_{0.9}O$ surface. In the previous publish [22], the PEC treatment technique have used to treat the ZnO surface, which could form the $Zn(OH)_2$ thin film on the ZnO surface. Therefore, the reduction of dark current was attributed to the fact that the PEC treatment could effectively diminish the number of dangling bonds on the $Mg_{0.1}Zn_{0.9}O$ surface. The photocurrent of the $Mg_{0.1}Zn_{0.9}O$ MSM-UPDs

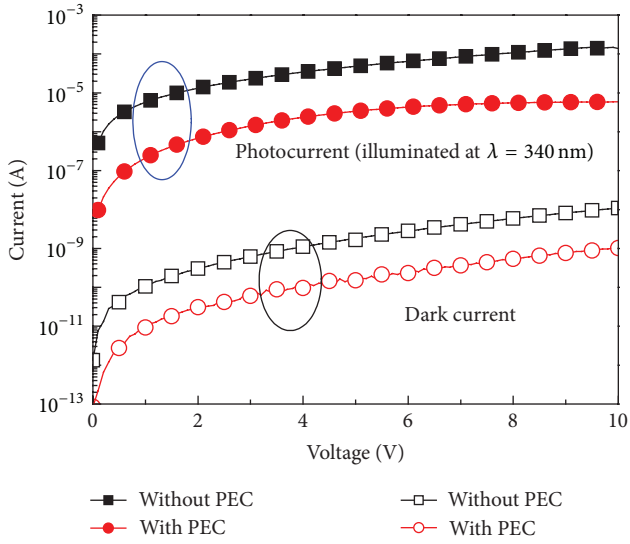

FIGURE 3: The current-voltage characteristics of the $Mg_{0.1}Zn_{0.9}O$ MSM-UPDs with and without PEC treatment.

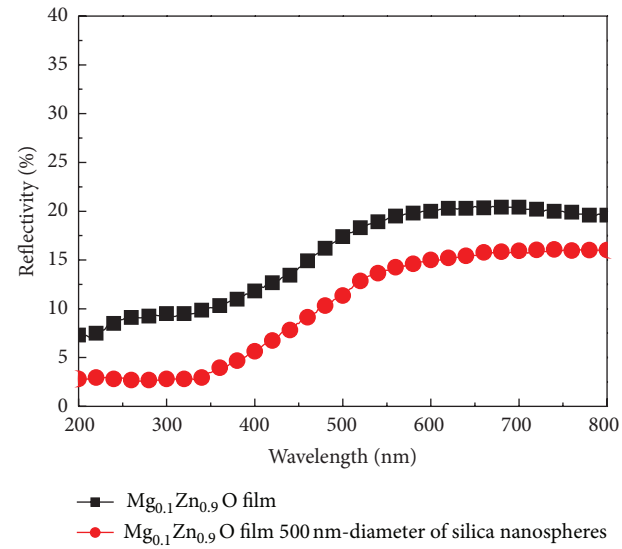

FIGURE 4: Reflectivity spectra of the $Mg_{0.1}Zn_{0.9}O$ films with and without 500 nm-diameter silica nanospheres.

with and without PEC treatment illuminated by a UV light with a wavelength of 340 nm was also measured and is shown in Figure 3 was also measured and is shown in Figure 3. The photocurrent of the unpassivated $Mg_{0.1}Zn_{0.9}O$ MSM-UPDs was larger than the passivated $Mg_{0.1}Zn_{0.9}O$ MSM-UPDs for all applied voltages. The photoinduced holes were trapped and accumulated between the active layer and cathode of the photodetectors due to the presence of defects on the active layer surface [23, 24]. Therefore, the internal gain of the unpassivated $Mg_{0.1}Zn_{0.9}O$ MSM-UPDs was caused by photoinduced holes accumulation, which reduced the Schottky barrier height between metal and $Mg_{0.1}Zn_{0.9}O$ film. Consequently, the higher photocurrent was attributed to the internal gain caused in the unpassivated $Mg_{0.1}Zn_{0.9}O$ MSM-UPDs.

To enhance the amount of incident light upon the $Mg_{0.1}Zn_{0.9}O$ MSM-UPDs, the 500 nm-diameter silica nanospheres were spin-coated to form a single layer as the antireflection layer on the $Mg_{0.1}Zn_{0.9}O$ MSM-UPDs. The optimal effective refractive index of the antireflection layer (n_{AR}) was estimated by the formula $n_{AR} = \sqrt{n_{air} \times n_{Mg_{0.1}Zn_{0.9}O}}$, where n_{air} of 1.00 and $n_{Mg_{0.1}Zn_{0.9}O}$ of 2.30 were the refractive indices of air and $Mg_{0.1}Zn_{0.9}O$ at wavelength of 340 nm, respectively. The solution of the optimal effective refractive index of the antireflection layer was 1.51. In this work, the effective refractive index of the silica nanospheres was measured by an ellipsometer and the value was about 1.48 which was similar to the optimal effective refractive index of the antireflection layer. Figure 4 shows the reflectivity of the $Mg_{0.1}Zn_{0.9}O$ films with and without silica nanospheres antireflection layer. As shown in Figure 4, the reflectivity of the $Mg_{0.1}Zn_{0.9}O$ films without and with silica nanospheres was 9.9% and 2.9% at the wavelength of 340 nm, respectively. Therefore, it was confirmed that the silica nanosphere was suitable to be used to form antireflection layer in the $Mg_{0.1}Zn_{0.9}O$ MSM-UPDs, which leaded more UV light to incident into the $Mg_{0.1}Zn_{0.9}O$ MSM-UPDs.

To exhibit the effect of the silica nanospheres antireflection layer on the photoresponsivity of the MSM-UPDs, the spectral photoresponsivity of passivated $Mg_{0.1}Zn_{0.9}O$ MSM-UPDs without and with antireflection layer is shown in Figures 5(a) and 5(b), respectively. The I-V characteristics of passivated $Mg_{0.1}Zn_{0.9}O$ MSM-UPDs without and with antireflection layer are shown in the inset of Figures 5(a) and 5(b), respectively. At bias voltage of 5 V, the photocurrent of passivated $Mg_{0.1}Zn_{0.9}O$ MSM-UPDs with antireflection layer illuminated by the UV light (wavelength = 340 nm and power = 40 μW) increased from 3.37 μA to 5.85 μA in comparison with passivated $Mg_{0.1}Zn_{0.9}O$ MSM-UPDs without antireflection layer. Besides, the UV-visible rejection ratio (R_{340}/R_{450}) of passivated $Mg_{0.1}Zn_{0.9}O$ MSM-UPDs with antireflection layer was increased from 5.50×10^3 to 1.44×10^4. The enhancements in the photocurrent and the UV-visible rejection ratio of the MSM-UPDs were attributed to that the amount of the incident light was enhanced by the antireflection layer, which could induce more electron-hole pairs in the active layer.

To investigate the detectivity performance of the $Mg_{0.1}Zn_{0.9}O$ MSM-UPDs without and with PEC passivation and antireflection layer, the noise power density of $Mg_{0.1}Zn_{0.9}O$ MSM-UPDs without and with PEC passivation and antireflection layer as a function of frequency is shown in Figures 6(a) and 6(b), respectively. The frequency range is from 1 Hz to 1000 Hz. Obviously, the fitting curve of noise power density spectra for both MSM-UPDs was similar to $1/f^2$, as shown in Figures 6(a) and 6(b). This result indicated that the dominant noise of the $Mg_{0.1}Zn_{0.9}O$ MSM-UPDs was the generation-recombination noise, which implied that the presence of generation-recombination centers is caused by the carrier trapping in the device [25]. Consequently,

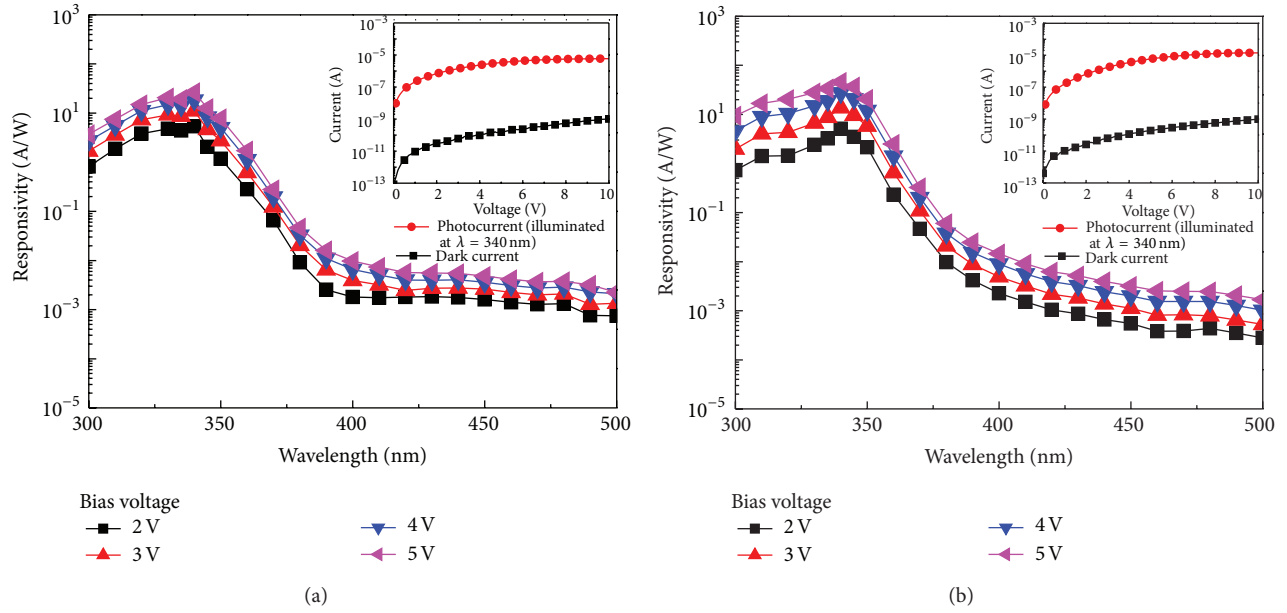

FIGURE 5: Photoresponsivity spectra of passivated $Mg_{0.1}Zn_{0.9}O$ MSM-UPDs (a) without and (b) with antireflection layer under various biases. The inset shows dark current and photocurrent versus bias voltage.

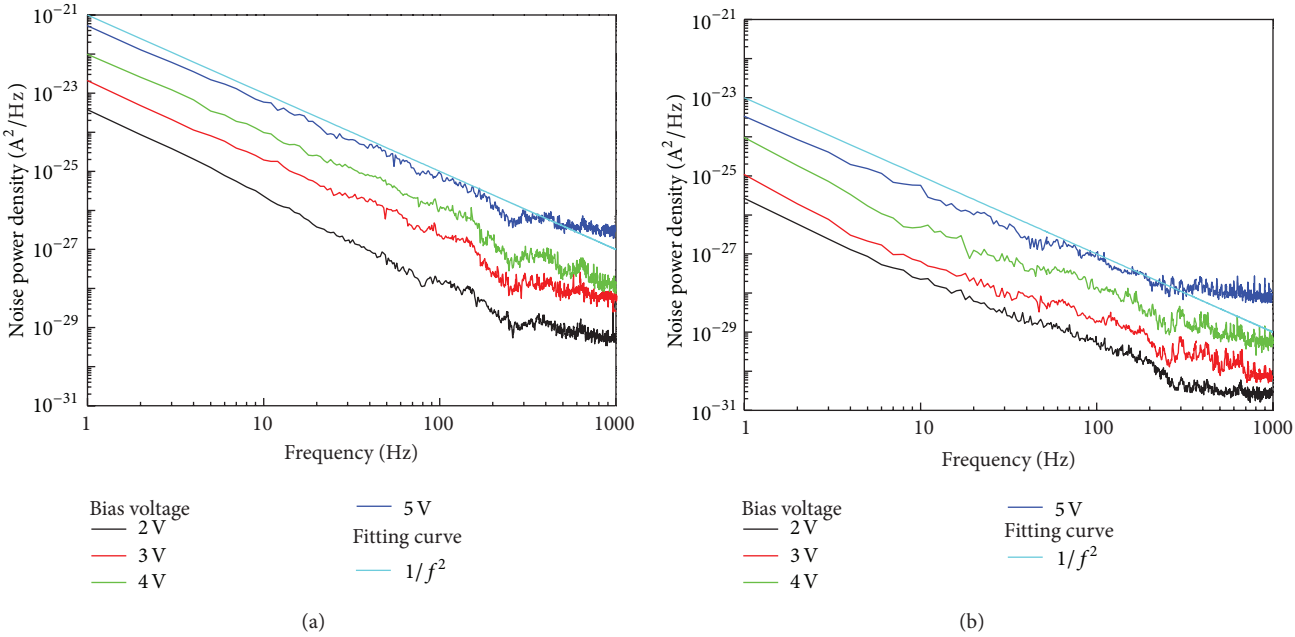

FIGURE 6: Noise power densities of the $Mg_{0.1}Zn_{0.9}O$ MSM-UPDs (a) without and (b) with PEC passivation and antireflection layer as a function of frequency for various bias voltages.

there was some generation-recombination centers existed in the $Mg_{0.1}Zn_{0.9}O$ films deposited by ALD system. In general, the noise equivalent power (NEP) and detectivity are commonly used to characterize the performance of the photodetector. The NEP was determined by the formula of NEP $= \sqrt{\langle I_n^2 \rangle}/R$, where $\langle I_n^2 \rangle$ is the mean square noise current and R is the photoresponsivity of MSM-UPDs. The specific detectivity (D^*) is defined as $D^* = \sqrt{A\Delta f}/\text{NEP}$, where A is the optical sensitive area of the photodetectors and Δf is the bandwidth of 1000 Hz [25]. As shown in Figures 6(a) and 6(b), at bias voltage of 5 V, the NEP of the $Mg_{0.1}Zn_{0.9}O$ MSM-UPDs without and with PEC passivation and antireflection layer was 6.18×10^{-13} W and 2.60×10^{-13} W and the corresponding D^* was 5.11×10^{11} cmHz$^{1/2}$W^{-1}

and 1.21×10^{12} cmHz$^{1/2}$W^{-1}, respectively. These results mentioned above confirmed that the PEC treatment and antireflection layer improved the performances of the $Mg_{0.1}Zn_{0.9}O$ MSM-UPDs. The improvement mechanism can be attributed to the excellent antireflection capability and effective passivation of dangling bonds on the surface of the $Mg_{0.1}Zn_{0.9}O$ films.

4. Conclusions

In this work, the PEC treatment and the antireflection layer were applied in the $Mg_{0.1}Zn_{0.9}O$ MSM-UPDs to enhance the performance. Since some dangling bonds remained on the $Mg_{0.1}Zn_{0.9}O$ surface after the ALD deposited process, the PEC treatment would passivate the $Mg_{0.1}Zn_{0.9}O$ surface by forming a $Zn(OH)_2$ thin film and the dark current of the passivted $Mg_{0.1}Zn_{0.9}O$ MSM-UPDs decreased about one order in comparison with unpassivated $Mg_{0.1}Zn_{0.9}O$ MSM-UPDs. In addition, the antireflection layer was constructed by coating 500 nm-diameter silica nanospheres on the $Mg_{0.1}Zn_{0.9}O$ films. The reflectivity of the $Mg_{0.1}Zn_{0.9}O$ film with silica nanospheres antireflection layer decreased to about 7.0% at the wavelength of 340 nm. Besides, the passivated $Mg_{0.1}Zn_{0.9}O$ MSM-UPDs with antireflection layer were fabricated and characterized. Compared with the passivated $Mg_{0.1}Zn_{0.9}O$ MSM-UPDs without antireflection layer, the photocurrent and UV-visible ratio of passivated $Mg_{0.1}Zn_{0.9}O$ MSM-UPDs with antireflection layer were enhanced to 5.85 μA and 1.44×10^4, respectively. The enhancements in the photocurrent and the UV-visible rejection ratio were attributed to the presence of the antireflection layer which effectively lead more UV light to incident into the active layer. Finally, the noise equivalent power of 2.60×10^{-13} W and the specific detectivity of 1.21×10^{12} cmHz$^{1/2}$W^{-1} for the passivated $Mg_{0.1}Zn_{0.9}O$ MSM-UPDs with antireflection layer had improved under a bias voltage of 5 V. The PEC passivation and silica nanospheres antireflection layer effectively enhanced the detectivity performance of $Mg_{0.1}Zn_{0.9}O$ MSM-UPDs, and it is promising the future application of UV photodetector.

Conflict of Interests

The authors declare that there is no conflict of interests regarding the publication of this paper.

Acknowledgments

This work was supported by the National Sciences Council of Taiwan under Grant NSC 101-2923-E-006-002-MY3 and NSC 102-2923-E-006-001-MY3 and the Advanced Optoelectronic Technology Center, National Cheng Kung University, Taiwan.

References

[1] Q. Zheng, F. Huang, K. Ding et al., "MgZnO-based metal-semiconductor-metal solar-blind photodetectors on ZnO substrates," *Applied Physics Letters*, vol. 98, no. 22, Article ID 221112, pp. 221112-1–221112-3, 2011.

[2] M. Liao and Y. Koide, "High-performance metal-semiconductor-metal deep-ultraviolet photodetectors based on homoepitaxial diamond thin film," *Applied Physics Letters*, vol. 89, no. 11, Article ID 113509, pp. 113509-1–113509-3, 2006.

[3] L. Sun, J. Chen, J. Li, and H. Jiang, "AlGaN solar-blind avalanche photodiodes with high multiplication gain," *Applied Physics Letters*, vol. 97, no. 19, Article ID 191103, pp. 191103-1–191103-3, 2010.

[4] D. X. Zhao, Y. C. Liu, D. Z. Shen, Y. M. Lu, J. Y. Zhang, and X. W. Fan, "Photoluminescence properties of $Mg_xZn_{1-x}O$ alloy thin films fabricated by the sol-gel deposition method," *Journal of Applied Physics*, vol. 90, no. 11, pp. 5561–5563, 2001.

[5] S. Fujita, H. Tanaka, and S. Fujita, "MBE growth of wide band gap wurtzite MgZnO quasi-alloys with MgO/ZnO superlattices for deep ultraviolet optical functions," *Journal of Crystal Growth*, vol. 278, no. 1–4, pp. 264–267, 2005.

[6] K. Ogata, K. Koike, T. Tanite et al., "ZnO and ZnMgO growth on *a*-plane sapphire by molecular beam epitaxy," *Journal of Crystal Growth*, vol. 251, no. 1–4, pp. 623–627, 2003.

[7] T. Gruber, C. Kirchner, R. Kling, F. Reuss, and A. Waag, "ZnMgO epilayers and ZnO-ZnMgO quantum wells for optoelectronic applications in the blue and UV spectral region," *Applied Physics Letters*, vol. 84, no. 26, pp. 5359-1–5359-3, 2004.

[8] K. Remashan, Y. S. Choi, S. J. Park, and J. H. Jang, "High performance MOCVD-grown ZnO thin-film transistor with a thin MgZnO layer at channel/gate insulator interface," *Journal of the Electrochemical Society*, vol. 157, no. 12, pp. H1121–H1126, 2010.

[9] H. Y. Lee, M. Y. Wang, K. J. Chang, and W. J. Lin, "Ultraviolet photodetector based on $Mg_xZn_{1-x}O$ thin films deposited by radio frequency magnetron sputtering," *IEEE Photonics Technology Letters*, vol. 20, no. 24, pp. 2108–2110, 2008.

[10] H. Y. Lee, H. Y. Chang, L. R. Lou, and C. T. Lee, "P-i-n MgBeZnO-based heterostructured ultraviolet LEDs," *IEEE Photonics Technology Letters*, vol. 25, no. 18, pp. 1770–1773, 2013.

[11] P. C. Wu, H. Y. Lee, and C. T. Lee, "Enhanced light emission of double heterostructured MgZnO/ZnO/MgZnO in ultraviolet blind light-emitting diodes deposited by vapor cooling condensation system," *Applied Physics Letters*, vol. 100, no. 13, Article ID 131116, pp. 131116-1–131116-3, 2012.

[12] S. Choopun, R. D. Vispute, W. Yang, R. P. Sharma, T. Venkatesan, and H. Shen, "Realization of band gap above 5.0 eV in metastable cubic-phase $Mg_xZn_{1-x}O$ alloy films," *Applied Physics Letters*, vol. 80, no. 9, pp. 1529–1531, 2002.

[13] A. I. Belogorokhov, A. Y. Polyakov, N. B. Smirnov et al., "Lattice vibrational properties of ZnMgO grown by pulsed laser deposition," *Applied Physics Letters*, vol. 90, no. 19, Article ID 192110, pp. 192110-1–192110-3, 2007.

[14] G. R. He and Y. J. Lin, "Current transport mechanism of heterojunction diodes based on the sol-gel p-type ZnO and n-type Si with H_2O_2 treatment," *Materials Chemistry and Physics*, vol. 136, no. 1, pp. 179–183, 2012.

[15] C. L. Tsai, Y. J. Lin, P. H. Wu et al., "Induced increase in surface work function and surface energy of indium tin oxide-doped ZnO films by $(NH_4)_2S_x$ treatment," *Journal of Applied Physics*, vol. 101, no. 11, Article ID 113713, pp. 113713-1–113713-4, 2007.

[16] C. T. Lee, Y. S. Chiu, S. C. Ho, and Y. J. Lee, "Investigation of a photoelectrochemical passivated ZnO-based glucose biosensor," *Sensors*, vol. 11, no. 5, pp. 4648–4655, 2011.

[17] C. Y. Tseng, C. K. Lee, and C. T. Lee, "Performance enhancement of III–V compound multijunction solar cell incorporating transparent electrode and surface treatment," *Progress in Photovoltaics*, vol. 19, no. 4, pp. 436–441, 2011.

[18] C. Y. Tseng, C. S. Lee, H. Y. Shin, and C. T. Lee, "Investigation of surface passivation on gaas-based compound solar cell using photoelectrochemical oxidation method," *Journal of the Electrochemical Society*, vol. 157, no. 7, pp. H779–H782, 2010.

[19] T. Glaser, A. Ihring, W. Morgenroth, N. Seifert, S. Schröter, and V. Baier, "High temperature resistant antireflective moth-eye structures for infrared radiation sensors," *Microsystem Technologies*, vol. 11, no. 2-3, pp. 86–90, 2005.

[20] M. Ibn-Elhaj and M. Schadt, "Optical polymer thin films with isotropic and anisotropic nano-corrugated surface topologies," *Nature*, vol. 410, no. 6830, pp. 796–799, 2001.

[21] B. T. Liu and W. D. Yeh, "Antireflective surface fabricated from colloidal silica nanoparticles," *Colloids and Surfaces A*, vol. 356, no. 1–3, pp. 145–149, 2010.

[22] H. Y. Lee, C. T. Lee, and J. T. Yan, "Emission mechanisms of passivated single n-ZnO:In/i-ZnO/p-GaN- heterostructured nanorod light-emitting diodes," *Applied Physics Letters*, vol. 97, no. 11, Article ID 111111, pp. 111111-1–111111-3, 2010.

[23] M. Klingenstein, J. Schneider, C. Moglestue et al., "Photocurrent gain mechanisms in metal-semiconductor-metal photodetectors," *Solid-State Electronics*, vol. 37, no. 2, pp. 333–340, 1994.

[24] H. Jiang, N. Nakata, G. Y. Zhao et al., "Back-illuminated GaN metal-semiconductor-metal UV photodetector with high internal gain," *Japanese Journal of Applied Physics 2*, vol. 40, no. 5, pp. L505–L507, 2001.

[25] C. H. Chen and C. T. Lee, "High detectivity mechanism of ZnO-based nanorod ultraviolet photodetectors," *IEEE Photonics Technology Letters*, vol. 25, no. 4, pp. 348–351, 2013.